XII International Conference on Computational Plasticity. Fundamentals and Applications
COMPLAS XII
E. Oñate, D.R.J. Owen, D. Peric and B. Suárez(Eds)

3D-MESOMECHANICAL ANALYSIS OF CRACKING AND SPALLING OF CONCRETE SUBJECT TO HIGH TEMPERATURES

A. PÉREZ, M. RODRIGUEZ, C.M. LÓPEZ AND I.CAROL

Department of Geotechnical Engineering and Geo-Sciences
ETSECCPB (School of Civil Engineering)-UPC (Technical Univ. of Catalonia), 08034 Barcelona
E-mail: adria.perez@upc.edu, mariana.rodriguez@upc.edu, carlos.maria.lopez@upc.edu, ignacio.carol@upc.edu

Keywords:2D and 3D Thermo-Meso-mechanical Analysis, High Temperature effect in concrete, Finite element method, Interface element.

Abstract. In this paper, an existing meso-structural model for concrete which had been applied to the study of the mechanical effects of high temperatures in 2D, is extended to 3D, and to more complex coupled thermo-mechanical analysis. The material is idealized as a two-phase compositein which all mesh lines (or surfaces in 3D) are potential cracks equipped with fracture-based zero-thickness interface elements. Different thermal expansion laws are assumed for matrix and particles, whereby the deformation mismatch can generate cracking. Temperature distributions are obtained from a separate thermal diffusionanalysis.The thermal analysis is first assumed uncoupled, but then also coupled with the mechanical analysis, as the layers of material spalloff and the boundary conditionsare moved to the new domain boundaries. The new computational results in 3D are compared to basic experimental observations reported in the literature and to the previous computational results obtained in 2D.

1 INTRODUCTION

The effects of temperature changes on heterogeneous materials such as concrete, may include internal stresses, cracking and degradation, even if the temperature distributions remain constant. This is due to the expansion mismatch between components. These effects may be investigated accurately only by considering explicitly the material meso-structure, that is, by representing the main material heterogeneities with their detailed (or at least approximate) geometry and applying to each of them the appropriate thermal expansion and material behavior laws. This approach has been consistently pursuedby the group of Mechanics of Materials UPC for the past 15 years, by considering a concrete model generated numerically, which was originally 2D and subject to mechanical loads [1], and then extended to 3D [2], and to more complex coupled environmental phenomena such as drying shrinkage or sulfate attack [3, 4]. In recent years, the approach has also been extended further to the effects of high temperature by deformation mismatch, caused by uniform and non-uniform temperature distributions applied according to the normalized ISO heating curve, which were applied onto the 2D specimens for both load-free and uniaxial compression loading situations [5-7]. In all those studies, however, the thermal analysis was totally uncoupled from the

mechanical analysis, that is, temperature distributions were computed beforehand once and for all the time increments, and were then imposed as a prescribed action to the mechanical calculation.

In this paper, these recent studies are extended to two new situations: 2D thermo-mechanical coupled analysis, and 3D. The cause of coupling in this case is the thermal boundary conditions: for the first time step temperature distributions are computed with the boundary conditions applied on the original specimen boundary. But this situation changes as the time goes on and layers of material start spalling off. Then, the new temperature b.c.s for each time increment are applied onto the newupdated domain boundaries.

2 MESOMECHANICAL MODEL

The numerical simulation is based on a meso-structural model in which the largest aggregate particles are represented explicitly, surrounded by a homogeneous matrix representing the average behavior of mortar plus the smaller aggregates. In order to capture the main potential crack trajectories, zero-thickness interface elements are inserted a priori of the analysis, along all the aggregate-mortar and some of the mortar-mortar mesh lines. These interface elements are equipped with a nonlinear constitutive law based on elasto-plasticity and concepts of fracture mechanics, which is formulated in terms of normal and shear components of the stress on the interface plane and the corresponding relative displacement variables. The initial loading (failure) surface $F = 0$ is given as three-parameters hyperbola (tensile strengthχ, asymptotic cohesion c and asymptotic friction angle $\tan\phi$). The evolution of F (hardening-softening laws), is based on the internal variableW_{cr}(work spent in fracture processes), with the two material parameters$G_F^I$and G_F^{IIa} that represent the classical fracture energy in Mode I, plus a second fracture energy for an "asymptotic" Mode IIa under shear and high confinement. A more detailed description of this elasto-plastic constitutive law can be found in the literature[8, 9]. Results of the meso-mechanical model for normal concrete specimens subject to a variety of loading cases in 2D and 3D can also be found elsewhere[2, 9-11]. For the current study, some of the 2D FE meshes used previously have been modified in the sense of adding some interface elements along mesh lines perpendicular to the aggregate surfaces at mid-distance between aggregate corners. In this way, the medium surrounding the expanding aggregate particle can crack in the direction that is more physical, and possible spurious tensile stresses in the surrounding material are minimized.

3 RESULTS OF 2D THERMO MESOMECHANICAL ANALYSIS

The time-dependent imposed temperature values correspond to the standard curve given in the fire-resistance tests recommendation ISO 834 [12], which are defined by equation 1 and plotted in Figure 1:

$$T = 345 Log10(8t + 1) + 20 \quad (1)$$

where T is the temperature in ºC and t is the time in minutes.In the numerical analysis, concrete is represented by large aggregates particles of dolomite rock surrounded by a matrix that represents mortar and smaller aggregates. The specimen considered has dimensions 10x10cm^2 and 10x30cm^2, volume fraction of large aggregates 28% and maximum aggregate

size 14mm (average aggregate size 10.4mm). The material parameters are: E = 70000 MPa (dolomite rock), E = 29000 MPa (mortar) and υ = 0.2 (both); for dolomite aggregate-mortar interfaces $K_N = K_T$ = 500000 MPa/mm, $tan\phi_0$= 0.90, χ_0 =4 MPa, c_0 = 15MPa, G^F_I = 0.025 N·mm, G^F_{II} = 10 G^F_I, σ_{dil} = 40 MPa, α_d= -2, and for mortar-mortar interfaces: $K_N = K_T$ = 500000 MPa/mm, $tan\phi_0$ = 0.90, χ_0 =6 MPa, c_0 = 20MPa, G^F_I = 0.030 N·mm, G^F_{II} = 10 G^F_I, σ_{dil} = 40 MPa, α_d= -2.

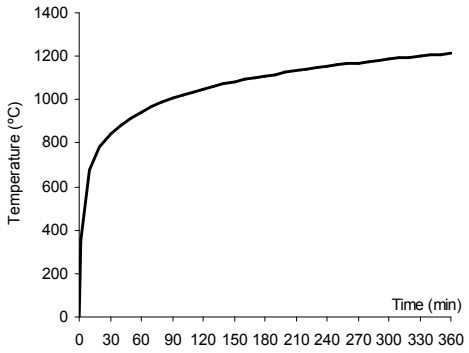

Figure 1:ISO 834 temperature-time curve (from [12]).

The thermal expansion parameters used are: for the matrix phase k = 0.66 J/min cm ºC; c_s = 1171J/kgºC and ρ = 0.0023 kg/cm3, and for the aggregate particles: k = 1.10 J/min cm ºC; c_s = 711J/kgºC and ρ = 0.0026 kg/cm3. The variable coefficient of thermal expansion for mortar is extracted from a volume expansion vs. temperature curve obtained numerically in [5]. For the aggregate a constant coefficient of thermal expansion extracted from the experimental results of Cruz and Guillen [13] who obtained independent expansion curves for aggregates, cement, mortarand concrete, are used (see Figure 2):

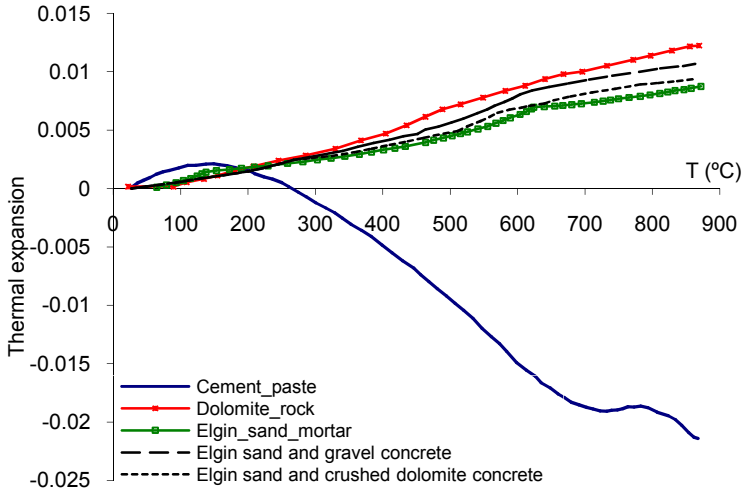

Figure 2: Experimental results for cement paste, dolomite rock, mortar and concrete (from Cruz & Gillen [13]).

3.1 2D analysis of a transversal section with non-uniform temperature distribution

For the sake of comparison, previous results presented in [7] are summarized in Figure 1. Assuming symmetry, a 40x40cm specimen cross-section was represented by the upper right 10x10cm one fourth. The temperature was applied on the upper and the right faces, while zero heat flow was imposed and normal displacement is restrained on the bottom and the left faces to simulate the symmetry conditions.

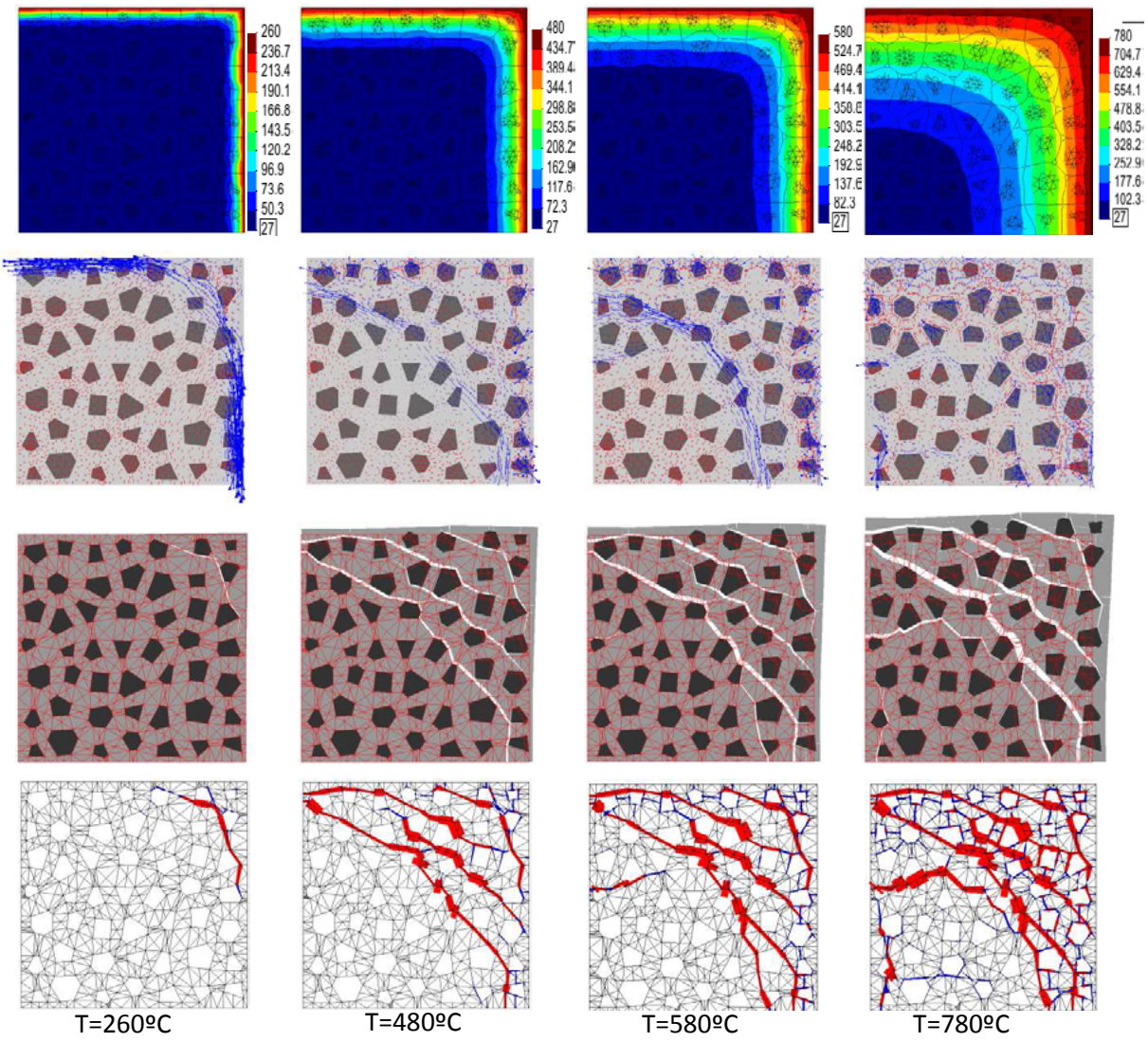

Figure 3: Evolution of temperature, continuum stress state, deformation and cracking in terms of the fracture energy (from top to bottom respectively) for the following four temperature values: T = 260, 480, 580 and 780ºC, corresponding for the following times: t = 0.50; 2.57; 5.12 and 19.82 minute.

Figure 3 shows the evolution for temperature, continuum stress state, deformation and cracking in terms of the fracture energy (from the top to bottom respectively) for four different temperature values: 260, 480, 580 and 780 ºC, which correspond to: 0.50; 2.57; 5.12 and 19.82 minutes after the beginning of the heating process. In the top row of the figure we

can see the temperature fronts that move into the specimen, not perfectly uniform due to the heterogeneities with different diffusivity coefficients.The second row depicts the evolution of the principal stresses, blue color for compression and red for tension, showing a front of compression stresses also moving into the specimen. Diagrams in the third row represent the deformed mesh with a magnification factor 10, and in the last row, the cracking state is represented in terms of the value W_{cr}/G_F^I (energy spent in the fracture process, over the fracture parameter in mode I), with blue color indicating values under 1.00 (i.e. cracking still in the process), and with red color indicating values over 1.00 (tensile crack open).

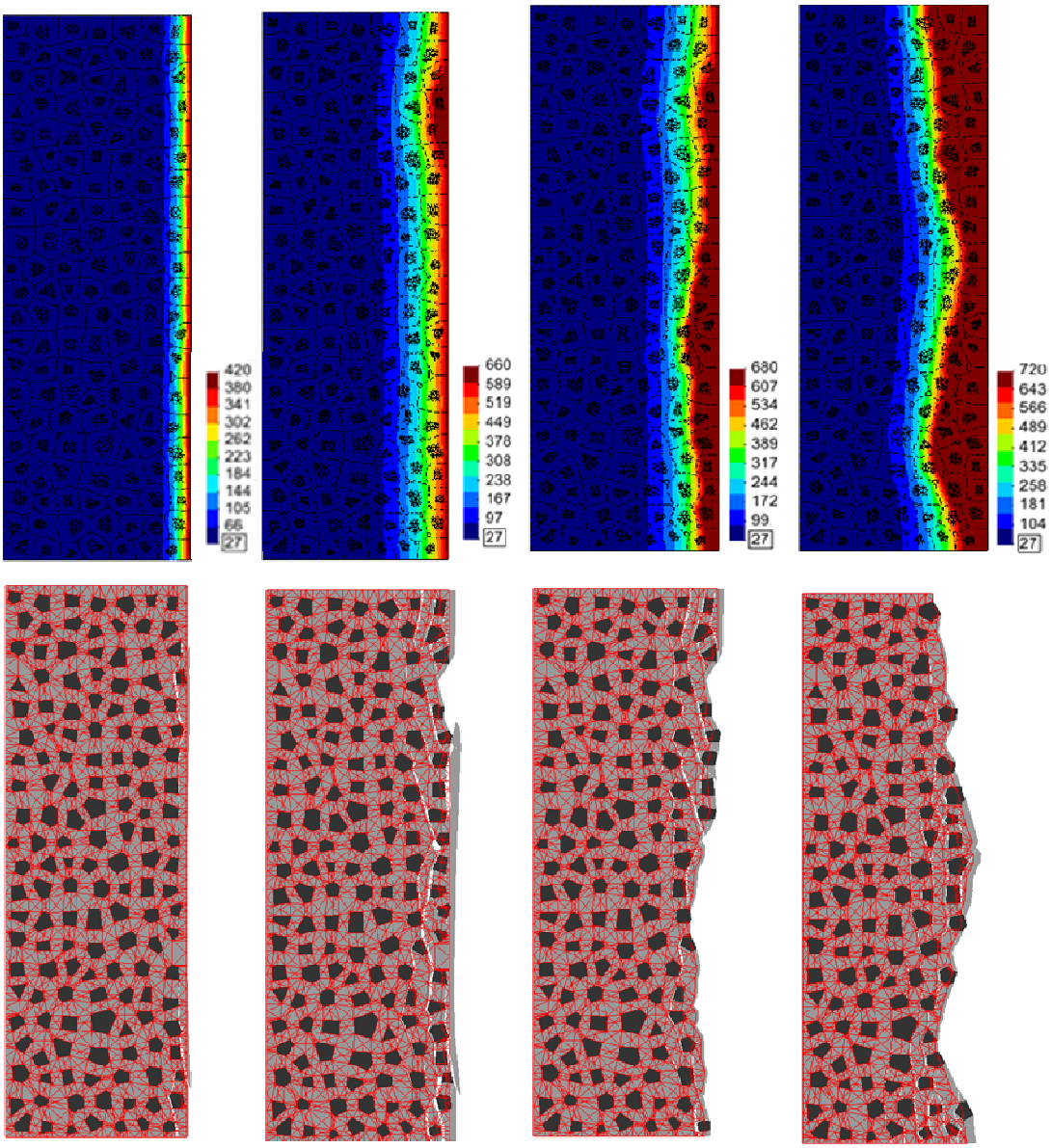

Figure 4: Evolution of temperature and deformation for the prescribed boundary values: T = 420, 660, 680 y 720ºC, corresponding to the ISO curve times: t = 1.68; 8.82; 10.10 and 13.23 minutes.

3.2 Coupled thermo-mechanical analysis with non-uniform distribution temperature

In this section a 10x30cm concrete specimen represents a section of a long wall subject to temperature increments according to the ISO 344 curve up to 720ºC, which are prescribed on the right vertical edge of the domain only, while thermal flow is assumed null on the other three faces. The displacements normal to the surface are also restrained along those faces.

Figure 4 depicts the temperature distribution (top) and cracking/spalling situation (bottom) obtained for four different calculation times, which correspond to prescribed temperatures of 420, 660, 680 y 720ºC, respectively. As already mentioned, the analysis includes the thermo-mechanical coupling due to the evolving geometry and boundary conditions of the thermal action, which, at each stage of the calculation are moved to the new boundary resulting from the mechanical spalling.

4 RESULTS OF 3D THERMO MESOMECHANICAL ANALYSIS

As a natural extension ofprevious studies, a full 3D analysis of the same problem has been undertaken. The preliminary results obtained in this study are presented in this section, including first the case with uniform temperature increments over the entire specimen, and then the case with a prescribed non-uniform temperaturedistribution obtained from a previous thermal analysis. In both cases the analysis is uncoupled, i.e. boundary conditions for the thermal analysis do not change in spite of the mechanical results, and therefore the thermal analysis can be performed entirely in advance, and the resulting temperature increments used as input for the mechanical analysis.

4.1 3D mechanical analysis with uniform temperature

In this simpler case all the nodes of the mesh are subjected to the same temperature value, which is increased stepwise from 27ºC to 867ºC. The interface and continuum parameters as well as the strategy used to perform the analysis, are the same as described in Section 3 for the 2D analysis, while thermal expansion values for each material component (mortar or aggregates) are extracted from the numerical curves shown in Figure 5of Ref. [5]. The 3D results are compared with the previous 2D results. The analysis is carried out for four specimens of different sizes and number of aggregates (9, 10, 16 and 32), whichexhibit the same volume fraction and the same maximum and average size of aggregatesas in the two dimensional analysis [5].

The 32-aggregate specimen includes 13683 continuum elements and 19887 interface elements, with a total of 38335 nodes and physical dimensions of 5x5x5 cm. The results for this specimen in terms of expansionsare depicted in Figure 5, with a curve that is remarkably similar to the one previously obtained in 2D with a 50-aggregate mesh [5], and shows a reasonable agreement with the experimental measurements [13].

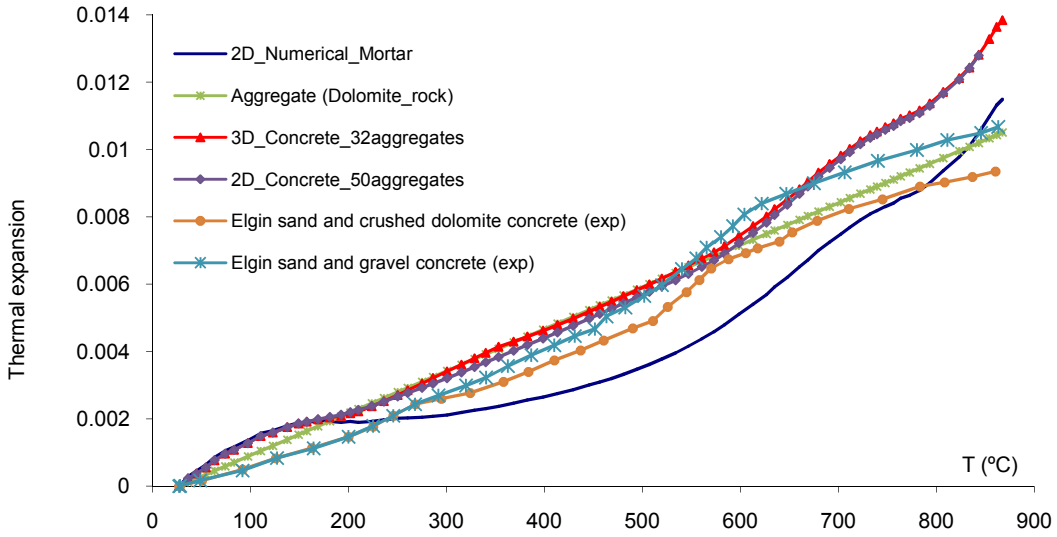

Figure 5: Thermal expansion of concrete under prescribed uniform temperatures: 3D numerical analysis (32-aggregate specimen),2D numerical results from [5], reference curves for aggregates and mortar from [5], and experimental results [13].

The expansion curves obtained for the various meshes with different number of aggregates are compared in Figure6,together with the curve that is obtained assuming elastic interfaces, that is if the cracks would not be allowed to open/slide (perfect bond). The latter is included in order to evaluate the effect of cracking on the overall specimen expansion.

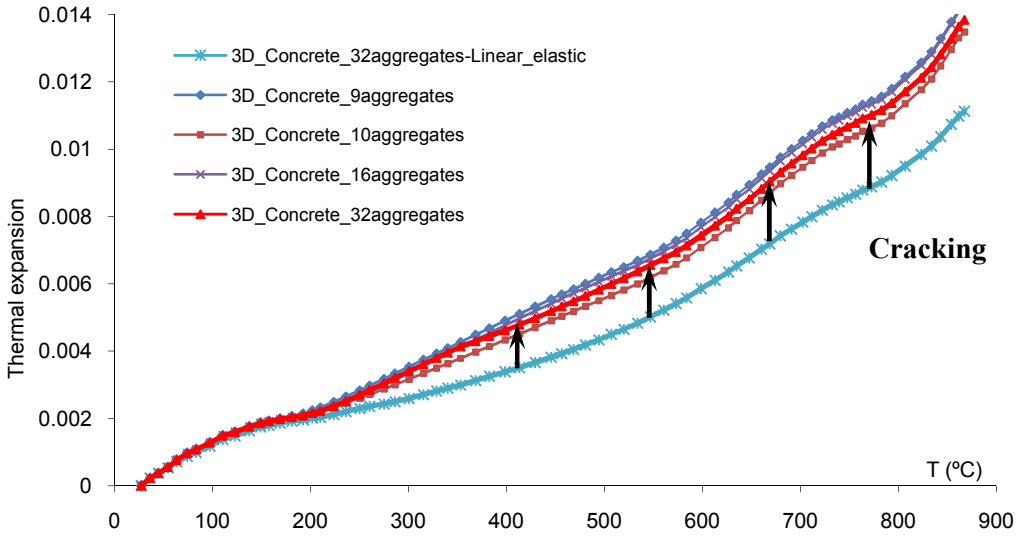

Figure 6: Non-linear numerical results for 3D concrete (9, 10, 16 and 32 aggregate specimen) and linear elastic numerical results for 3D concrete.

Finally, Figure 7 shows the evolution of the deformation for the 32-aggregate specimen, (magnification factor 120) for temperatures of 74, 328, 584 and 867ºC, and Figure 8 shows

the final deformation for the other three smaller meshes with 9, 10 and 16 aggregate pieces.

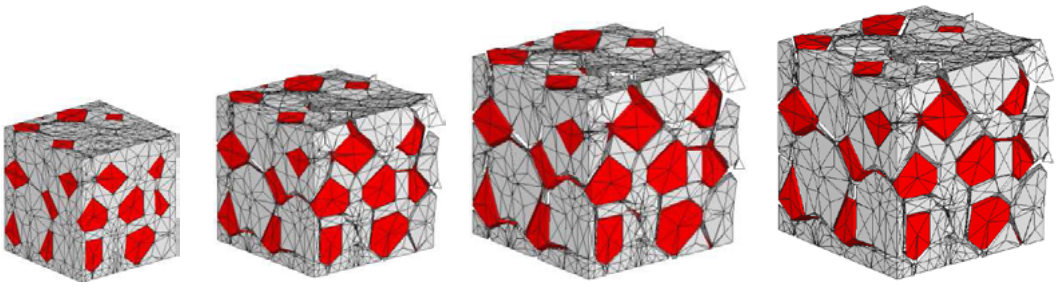

Figure 7: Evolution of deformation (x120) of the 32-aggregate mesh for the following four temperature values: T = 74, 328, 584 and 867ºC

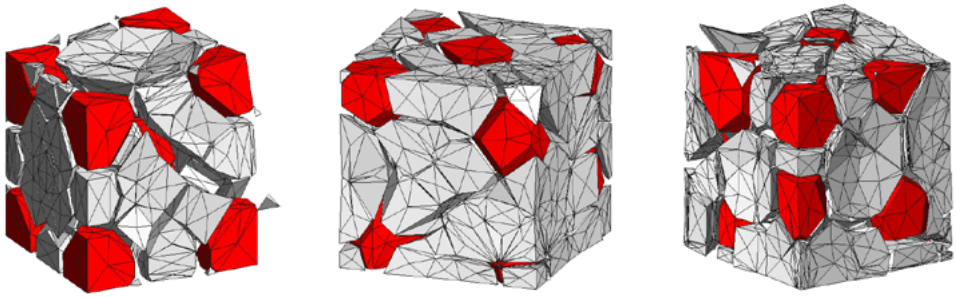

Figure 8: Finaldeformation (x120) of the 9, 10 and 16 aggregate specimens for a T = 867ºC.

4.2 3D thermo-mechanical analysis with non-uniform temperature distribution.

In this example, temperature is prescribed on one or more faces of the specimen, with increasing values according to the ISO834 standard curve of Figure 2 [12]. The parameters for interface and continuum elements used in this section, and the strategy to perform the analysis, are the same as described for the 2D case in section 3. This analysis is performed on two different geometries. First, a 4x4x6 cm specimen is assumed to represents one fourth of a column slice of 8x8x6 cm. The temperature is applied on two adjacent vertical faces, while zero heat flow is imposed and normal displacement is restrained on the other faces to simulate the symmetry conditions (Figure 9). The specimen, of 42 aggregates, includes 18518 continuum elements and 26698 interface elements, with a total of 51795 nodes.

The diagrams in the first row of Figure 9show the temperature fronts moving into the specimen at various times, which turn out slightly irregular due to material heterogeneities. Diagrams in the second row represent the evolution of the deformed mesh with a magnification factor 100. Cracking generated exhibits trends similar to those obtained in the corresponding 2D analysis (Figure 3).

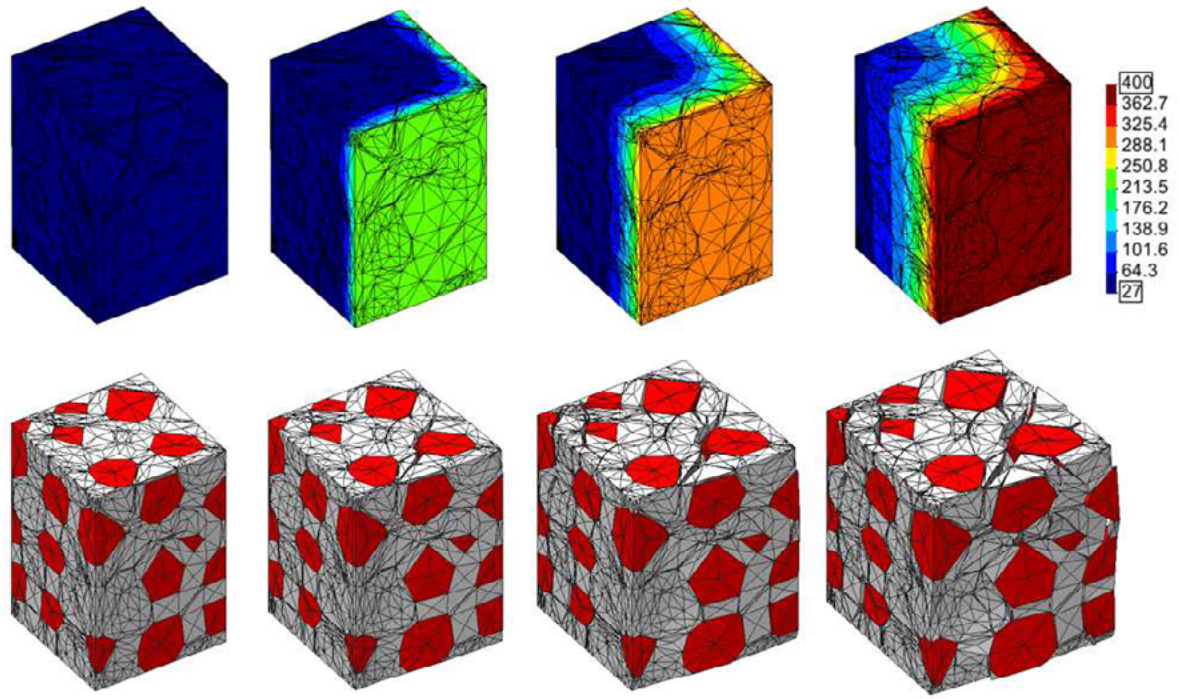

Figure 9: Results for the 42-aggregate specimen.Evolution of temperature (top), and deformation x100 (bottom diagrams) for four prescribed temperature values T = 27, 220, 300 and 400ºC, which correspondto the ISO834 heating times t = 0, 21, 41 and 87 seconds.

The second geometry is a 6x2.5x6 cm specimenrepresenting only a representative portion of alarge slab subject to thermal action on its surface.Temperature is applied on one of the larger vertical faces, while zero heat flow and zero normal displacements are imposed on the other faces to simulate the symmetry conditions (Figure 10). The specimen, of 35 aggregates, includes 18766 continuum elements and 27564 interface elements, with a total of 53521 nodes.

Figure 10 shows, as for the 42-aggregate mesh, the evolution of temperatures for different times and the equivalent deformation for each time with a magnification factor 120.

In both cases (Figures 9 and 10) it is observed that as the temperature fronts move inside the specimen, cracking develops with the trend to cause detachment of surface layers of material including the first line of aggregates.

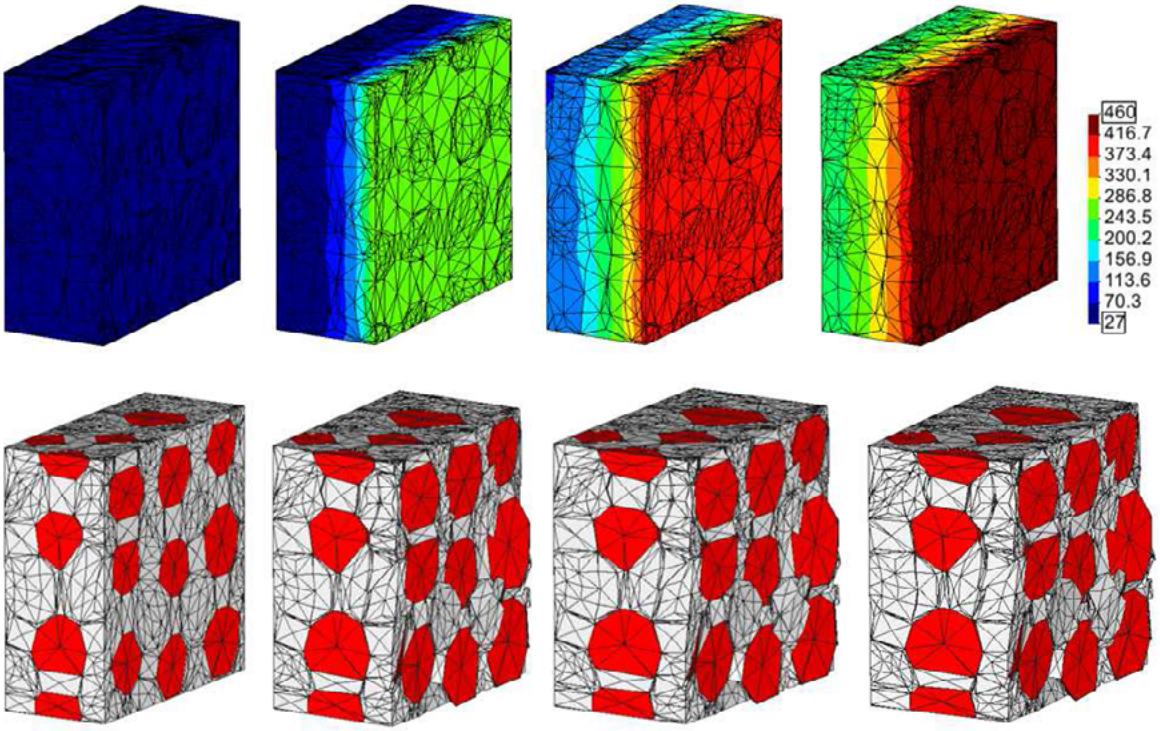

Figure 10: Results for the 35 aggregate specimen. Evolution of temperature, and deformation x120 (from top to bottom respectively) for the following four temperature values: T = 27, 280, 400 and 460ºC, corresponding for the following times: t = 0, 35, 87 and 134 seconds.

5 CONCLUDING REMARKS

The model proposed, based on a meso-level representation of the concrete material with potential cracks pre-inserted *via* zero-thickness interface elements with a fracture-based constitutive model, seems to lead to a realistic representation of the cracking and spalling phenomena related to the differential volume changes caused by high temperatures.2D and 3D calculations with the same approach, lead to results which are very close, even more considering the relatively coarse representations of the aggregate geometry. In all the cases analyzed, both in 2D (Figures 3 and 4) and 3D (Figures9 and 10), spalling is clearly observed, as the temperature fronts move inside the specimenand cracking develops with the trend to cause detachment of surface layers of material including the first line of aggregates.

Acknowledgements

This research has been supported partially by research project BIA2012-36898 funded by MEC (Madrid), which include FEDER founds, and 2009SGR-180 from AGAUR-Generalitat de Catalunya (Barcelona).

REFERENCES

[1] López, C.M. Análisis microestructural de la fractura del hormigón utilizando elementos finitos tipo junta. Aplicación a diferentes hormigones. *PhD thesis*, UPC, Barcelona, Spain (1999).
[2] Caballero, A., Carol, I., López C. M. 3D mesomechanical analysis of concrete specimens under biaxial loading. *Fatigue and Fracture Engng. Mat. and Structures*, 30, 877-886 (2007).
[3] Idiart, A.E., López, C.M and Carol, I. Modeling of drying shrinkage of concrete specimens at the meso-level. *Mat. and Structures,* 44:415-435 (2011).
[4] Idiart, A.E., López, C.M and Carol, I. Chemo-mechanical analysis of concrete cracking and degradation due to external sulfate attack:ameso-scale model.*Cement and Concrete Composites*, vol 33, pp. 411-423, (2011).
[5] Rodríguez, M., López, C.M., Carol, I., and Murcia, J. High temperature effects in mortar and concrete specimens using a meso-mechanical model with fracture based zero-thickness interface elements. *XI International Conference on Computational Plasticity Fundamentals and Applications*, Barcelona, Spain (2011).
[6] Rodríguez, M., López, C.M., Carol, I., and Willam, K.J.Meso-mechanical modeling of thermal spalling in concrete using fracture-base zero-thickness interface elements. *Proceeding of the 2nd International RILEM Workshop*, pp237-244, Delft, The Netherlands (2011).
[7] Rodríguez, M., López, C.M., and Carol, I.Meso-mechanical study of high-temperature cracking in mortar and concrete specimens using fracture-base zero-thickness interfaces. *Strategies for Sustainable Concrete Structures (SSCS),* pp. 1-9, Aix-en-Provence, France, (2012).
[8] Carol, I., Prat, P. C., López, C.M. A normal/shear cracking model.Application to discrete crack analysis.*Engng.Mech. ASCE*, 123, pp. 765–773 (1997).
[9] Carol, I., López, C.M. and Roa, O.Micromechanical analysis of quasi-brittle materials using fracture-based interface elements.*Int. J. Num. Meth. Engng.,*Vol 52, pag. 193-215 (2001).
[10] López C.M., Carol I., Aguado A.Meso-structural study of concrete fracture using interface elements. I: numerical model and tensile behaviour. *Materials and Structures*, Vol. 41, Nº 3, pag.583-599 (2008).
[11] López C.M., Carol I., Aguado A.Meso-structural study of concrete fracture using interface element II: compression, biaxial and Brazilian test.*Materials and Structures*, Vol. 41, Nº 3, pag.601-620 (2008).
[12] ISO834-1.Fire Resistance Test – Element of Building constructions- Part 1: General Requirement, (1999).
[13] Cruz, C. R., and Gillen, M.Thermal expansion of Portland cement paste, mortar and concrete at high temperatures. *Fire and materials*,vol.4 nº2, pp. 66-70 (1980).